Nonlinear Processes in Geophysics (1999) 6: 235–242

Nonlinear Processes in Geophysics

Energetic particle cross-field diffusion: Interaction with Magnetic Decreases (MDs)

B. T. Tsurutani[1], G. S. Lakhina[2], D. Winterhalter[1], J. K. Arballo[1], C. Galvan[1], and R. Sukurai[1]

[1]Jet Propulsion Laboratory, California Institute of Technology, Pasadena, CA 91109, USA
[2]Indian Institute of Geomagnetism, Colaba, Mumbai/Bombay, India

Received: 19 July 1999 – Revised: 20 September 1999 – Accepted: 8 October 1999

Abstract. Magnetic field Decreases (MDs) are detected in the heliospheric polar regions. The MDs have minimum spatial scales sizes of 25 proton thermal gyroradii, and are typically bounded by tangential or rotational discontinuities. The distribution of the magnitudes of the decreases within MDs is a continuum, with the smallest decreases being most frequent in occurrence. The largest decreases can be $\sim 80\%$ of the ambient field. The thickness distribution is also a continuum, and is shown to be independent of the field magnitude decrease. Charged particle interactions with the MDs lead to particle guiding center displacements and hence particle cross-field diffusion. We develop a diffusion model to apply to energetic ion interactions with MDs using the MD properties described in this paper. One specific day of data is used to illustrate that the particle cross-field diffusion will be extremely rapid due to such interactions.

1 Introduction

The Ulysses spacecraft passed over the polar region ($-80°$) of the heliosphere for the first time in August 1994. The distance from the sun was 2.3 AU. Subsequent reports of the plasma and magnetic field measurements demonstrated that this region was dominated by a high-speed ($\sim 750 - 800$ km s^{-1}) solar wind emanating from a polar coronal hole (Phillips et al., 1994). It was also shown that these streams contain large amplitude ($\Delta \vec{B}/B_0 \sim 1$ to 2), noncompressive Alfvén waves (Tsurutani et al., 1994, 1995; Smith et al., 1995a; Balogh et al., 1995; Goldstein et al., 1995).

The purpose of this paper is to demonstrate that there is another type of solar wind microstructure at high latitudes. The properties of these microstructures will be examined as well as the propagation and transport effects that these structures will have on energetic charged particles.

Correspondence to: Bruce T. Tsurutani

2 Results

2.1 Properties of Magnetic Decreases

Figure 1 is a plot of one month of magnetic field data centered at the highest latitude attained by Ulysses ($-80°$) at the south pole. The three magnetic field components are given in a SH coordinate system, where $\hat{r}$ is radially outward from the sun, $\hat{t} = (\hat{\Omega} \times \hat{r})/|\hat{\Omega} \times \hat{r}|$, $\hat{\Omega}$ is the rotation axis of the sun, and $\hat{n}$ forms the right-hand system. The field magnitude is given in the bottom panel.

The large amplitude fluctuations in the field components (the top three panels) are primarily associated with Alfvén waves. The x, y, and z components have ± 1 nT variations in a ~ 1.2 nT magnetic field, thus $\Delta \vec{B}/B_0 \sim 1$ to 2. The bottom panel shows the large magnetic field decreases that are the focus of this paper. The field occasionally decreases to 0.2 nT (the plots are one-minute averages) or $\Delta|B|/B_0 \sim 0.8$. For simplicity we call these phenomena Magnetic Decreases or MDs (Tsurutani and Ho, 1999).

Figure 2 illustrates several of the MDs in higher time resolution. Panel a) shows a magnetic field magnitude decrease on September 7, 1994 from $\sim$ 0942:40 to 0944:10 UT. The field decreases from ~ 1.5 nT to as low as 0.2 nT. The field decrease is bounded by two sharp discontinuities. This is often the case. The discontinuities have been analyzed using the minimum variance method applied to the highest time resolution data (2s). The normal direction of the first discontinuity is oriented at 80° relative to the ambient magnetic field. The normal direction of the second discontinuity is 90° relative to the ambient field. The maximum field magnitude changes are from 1.25 nT to 0.8 nT for the first event and from 1.25 nT to 0.2 nT for the second event. $\Delta|B|/B_0 = 0.35$ and 0.8, respectively. The discontinuities are thus tangential in nature.

To attempt to place the magnetic decrease in context with the overall solar wind/field structures, we note that an Alfvén wave (see B_r component) is present from 0935:00 to 0953:30 UT. There is a fast field rotation from 0951:30 to

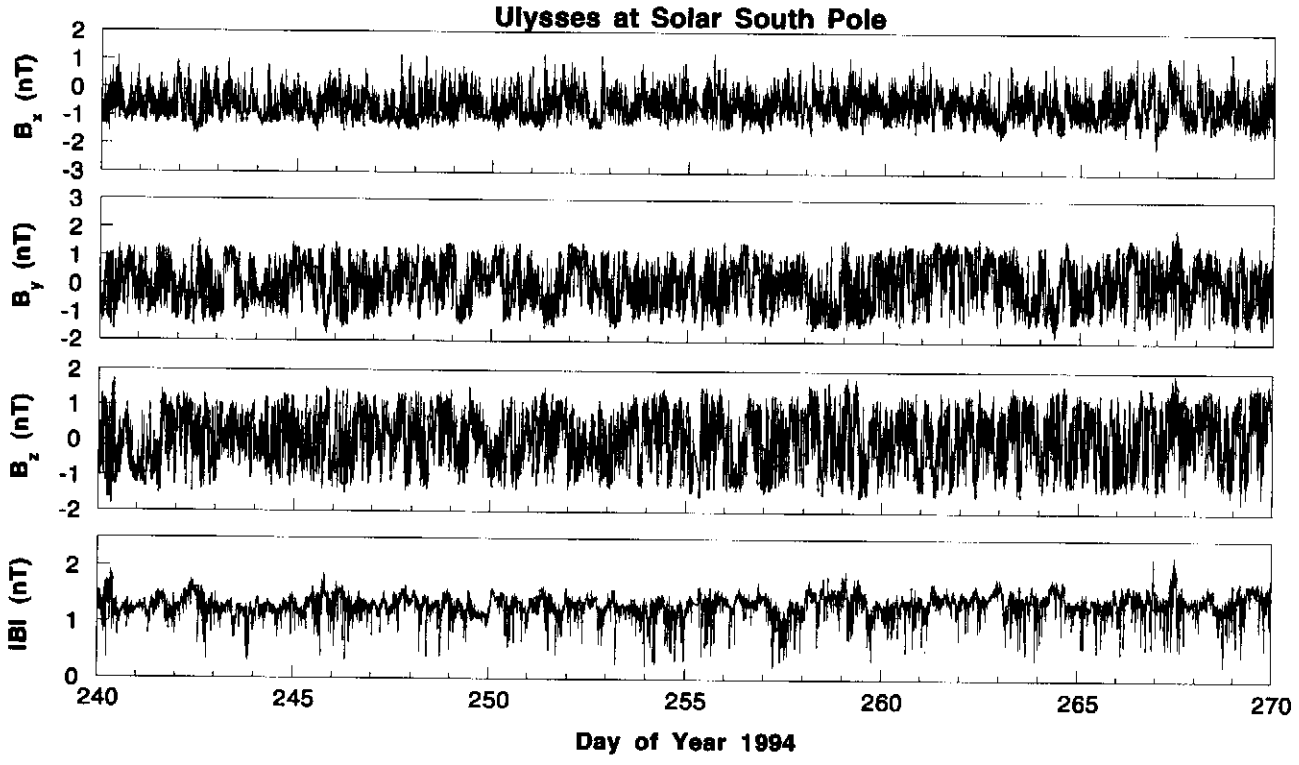

Fig. 1. The (south) polar magnetic field detected at 2.3 AU distance from the sun. The field is given in SH coordinates. The field magnitude plot illustrates the presence of frequent and large magentic field magnitude decreases (MDs).

$\sim$ 0953:30 UT at the edge of the wave. There is a similar, but smaller field decrease near the field rotation. The latter feature is associated with the termination of the Alfvén wave. The magnetic decrease of primary interest was located near the center of the Alfvén wave.

Figure 2b illustrates another type of MD on September 11, 1994. The three field components given in minimum variance coordinates are noted to rotate smoothly throughout the whole MD structure from $\sim$ 2151:40 UT to 2153 UT. The field is 1.4 nT prior to the decrease and 1.0 nT afterward. The magnetic field orientation changes significantly across the structure. The B_r component changes from $\sim +1.0$ nT to ~ -1.0 nT and B_n changes from -0.7 nT to $+0.2$ nT.

This MD is also bounded by sharp field magnitude decreases. The small discontinuity at 2151:40 UT has a normal component oriented $\sim 49°$ relative to $\vec{B}_0$. This appears to be a rotational discontinuity (RD) with a significant magnitude change (0.25 nT). The second discontinuity at $\sim$ 2153 UT has a normal $\theta_{Bn} = 77°$. For the latter event, the field magnitude changes from 1.0 nT to 0.45 nT, or $\Delta|B|/B_0 = 0.55$. This is a tangential discontinuity (TD).

The third example is given in Fig. 2c, from $\sim$ 0652:40 to 0655:05 UT, September 3, 1994. The decrease is sharp at both edges of the MD. The normal angle θ_{Bn} is 89° for the first discontinuity and 88° for the second. The field is 1.5 nT both prior to the MD and after the MD. The field decreases to 0.3 nT in the first discontinuity and to 0.45 nT in the second. Both discontinuities are clearly tangential in nature. Here the B_r component changes gradually across the MD. However the B_n component changes abruptly only at the second TD.

Table 1. Discontinuity thicknesses in time, kilometers, and proton gyroradii.

Year	Day	Start time (UT)	Stop time (UT)	Δt (s)	Thickness (km)	r_p
1994	246	0652:44	0652:52	8	666	1.5
1994	246	0655:02	0655:04	2	1275	3.0
1994	250	0942:47	0942:51	4	2538	5.9
1994	250	0944:03	0944:07	4	1308	3.0
1994	254	2151:39	2151:42	3	2178	5.1
1994	254	2152:50	2153:06	16	7476	17.4

The discontinuity thicknesses are given in Table 1. The thicknesses were calculated from the expression

$$l = V_{SW}\,\tau_{MD}\cos\theta_{nv} \qquad (1)$$

where V_{SW} is the measured solar wind velocity, τ_{MD} the measured "temporal thickness" of the discontinuity, and θ_{nv} the angle between the normal and the solar wind flow direction. The typical field magnitude was $\sim$ 1.2 nT and the proton temperature 1.5×10^5 K. The proton gyroradius is thus $\sim$ 430 km. The discontinuity thicknesses range from 1.5 to 17.4 times the proton thermal gyroradius.

Figure 3 gives the distribution of the field decreases within MDs. 129 MDs with field magnitude decreases of $> 20\%$ were examined. The field decreases are noted to be contin-

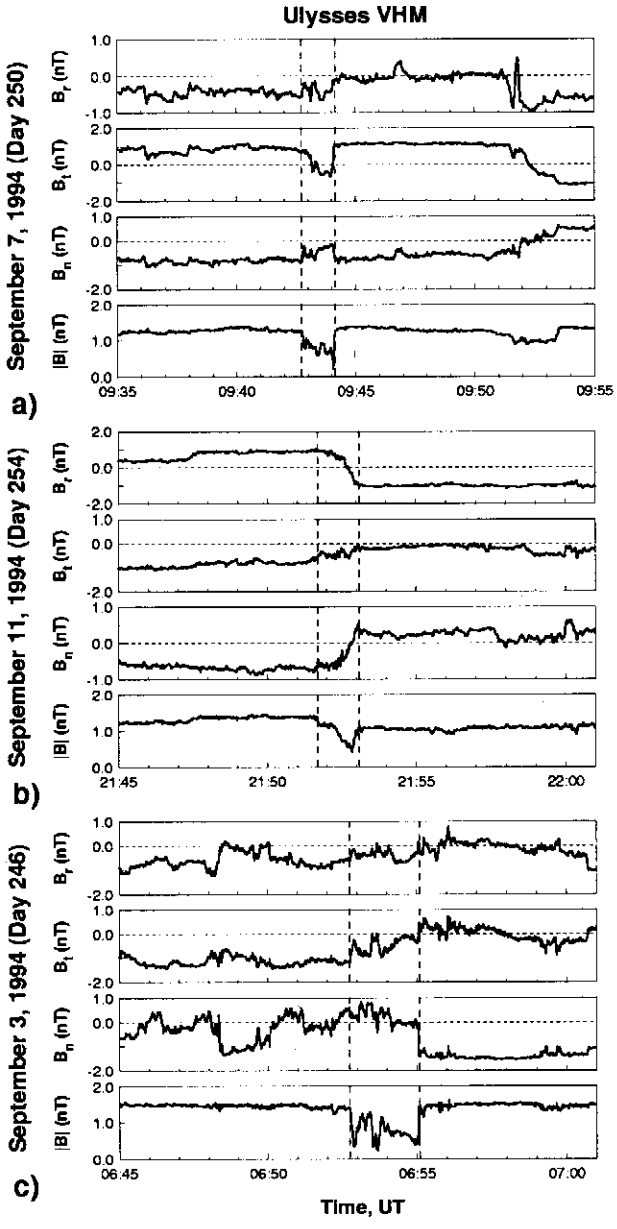

Fig. 2. Three MDs examined in high time resolution. The MDs are often (but not always) bounded by discontinuities with small normals (tangential discontinuities).

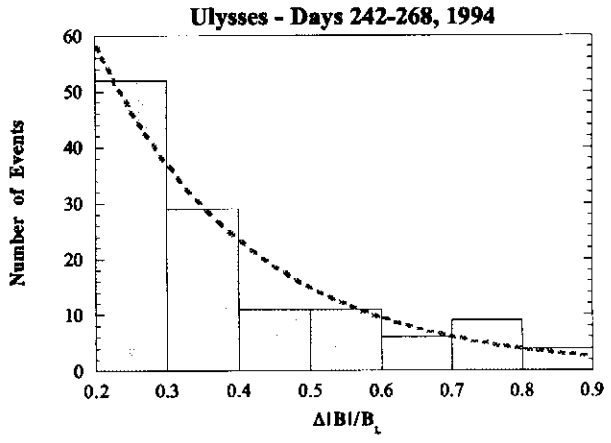

Fig. 3. Examination of all discontinuities with $\Delta|B|/B_L > 0.2$ bounding magnetic decreases in the interval Day 242 to 268, 1994. There are 129 events. The distribution is a continuum. There are fewer events with large B_N values.

uous, with the smallest decreases being the most common. The exponential fit is determined to be $129e^{-4\Delta|B|/B_L}$.

The distribution of the thicknesses for the MDs shown in Fig. 3 is given in Fig. 4. Forty-nine percent of all MDs have thicknesses less than 4×10^4 km. The percent occurrence falls off with increasing thickness. Again, using a proton gyroradius of ~ 430 km, the minimum thickness of the MDs is $25r_p$ (not shown). Thus, half of the MDs have thicknesses between 25 and $80r_p$.

Figure 5 shows the temporal thickness distributions for MDs with $20-30\%$, $30-40\%$, $40-50\%$ and $60-100\%$ decreases, respectively. The distributions are, to first order, the same. The MD thickness is, to first order, independent of the magnitude of the decrease. The fact that these two parameters are independent will make the modeling of particle interaction with MDs much simpler.

The normals to the discontinuities were calculated using minimum variance analyses. The jumps in field magnitude at

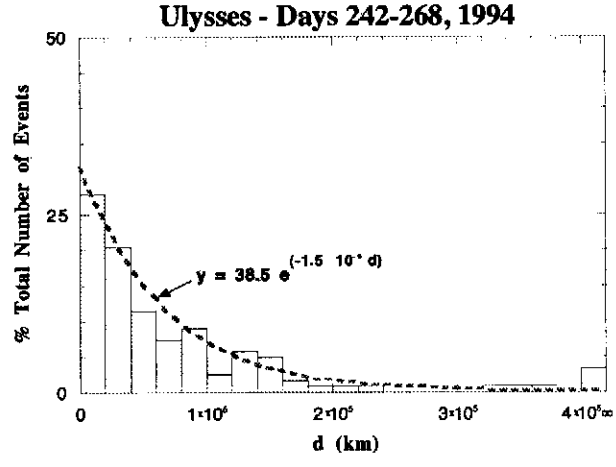

Fig. 4. The thickness distribution for different magnitude ranges of field decreases.

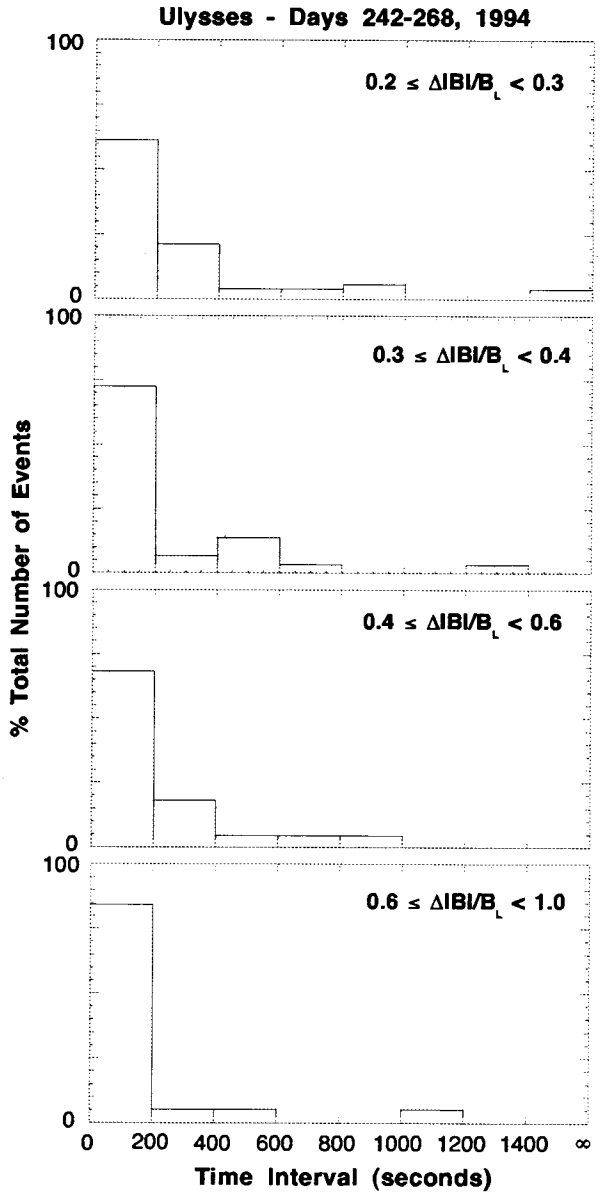

Fig. 5. The MD thickness distribution for different magnitude ranges of field decreases. Since the four distributions are similar, it is concluded that MD thickness is independent of the magnitude of the field decrease.

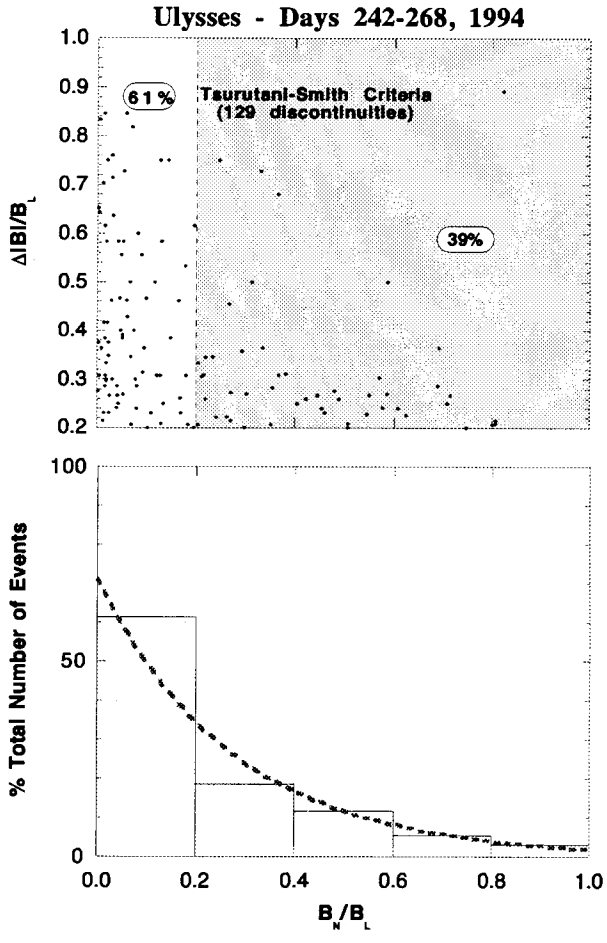

Fig. 6. MD field decrease as a function of discontinuity normal. MDs with the largest field decreases have the smallest normal field components.

the boundaries were also measured. The discontinuities are shown in Fig. 6 in phase space. B_L is the larger field magnitude on either side of the discontinuity. Discontinuities with small normals (left-hand portion of the panel) are tangential discontinuities (Smith, 1973; Tsurutani and Ho, 1999). Tangential discontinuities have the largest relative magnitude changes. Events with large field normals have smaller field magnitude changes. The discontinuity normals are a continuum. A histogram is shown at the bottom of the figure. The greatest number of discontinuities (49%) occurs where the normals are the smallest, and the least number when the normals are the largest. The fit is $90e^{-3.6(B_N/B_L)}$.

2.2 Particle-MD interactions

The previous statistical results of MD-properties will be useful to determine the mechanisms for the formation of MDs. The properties are also necessary to be able to model energetic particle interactions with such structures. In the following section we construct a particle cross-field diffusion model with the aid of some simplifying assumptions.

The mechanism for cross-field diffusion is a general one that can be applied to any place where there are relatively strong magnetic field gradients. Thus there are many space plasma and astrophysical applications for a generalization of the model. It should be noted that particle-MD interactions are substantially different than wave-particle interactions. Wave-particle interactions (for a detailed discussion, see Tsurutani and Lakhina (1997)) occur when propagating waves have resonant interactions with energetic particles. If the conditions for resonance are not met, the interaction is negligible. The primary results of such quasilinear diffusion models (see Schlickeiser (1989) and references therein) lead primarily to particle diffusion in pitch angle. Such interactions also lead to diffusion in energy space and in cross-field diffusion, but only as second order effects. On the other hand, MDs are most likely static structures that are convected by the solar wind. The interaction does not involve resonances.

Figure 7 illustrates the basic geometry of the interaction. The particle gyrates in a uniform magnetic field B_0 (into the paper) with gyroradius "r". The MD has a circular cross-section (a simplification) of radius "a". The field within the MD is in the same direction as the ambient magnetic field direction, but with reduced intensity. The "impact parameter", the distance from the center of gyration to the center of the MD is "d".

Figure 8 shows how the charged particle-MD interaction will move the particle guiding center perpendicular to the magnetic field. The particle has its guiding center at point O and the particle impacts the MD at point P_1. Due to the abrupt change in the magnetic field strength from B_0 to B_{MD}, the particle's first adiabatic invariant is broken and the gyrocenter becomes point O'. The new gyroradius r' is equal to $r\ (B_0/B_{MD})$. The particle exits the MD at point P_2 with a new guiding center located at point O''. Note that through this interaction the particle gyrocenter has moved from point

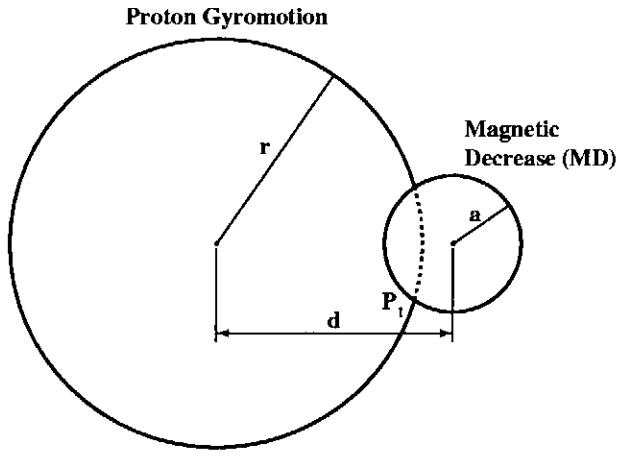

Fig. 7. Geometry of a charged particle gyromotion and a Magnetic Decrease. The impact parameter is "d".

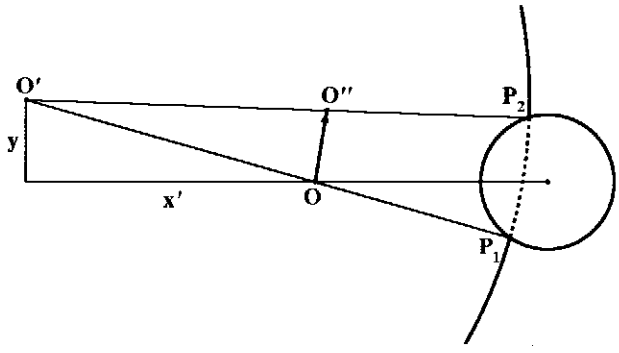

Fig. 8. Schematic showing cross-field motion of the gyrocenter of a charged particle from the interaction with a MD.

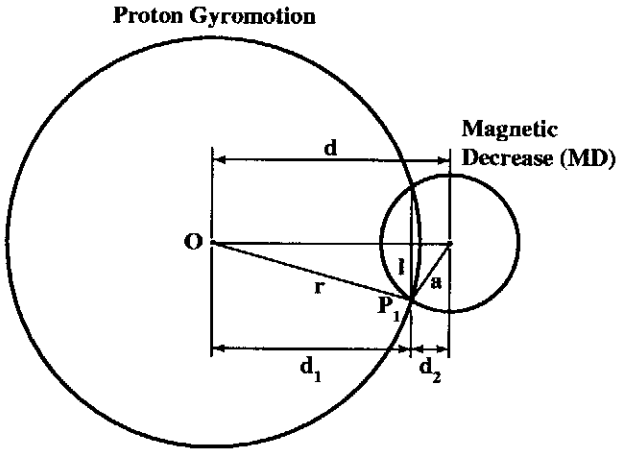

Fig. 9. Further geometry of a proton-MD interaction.

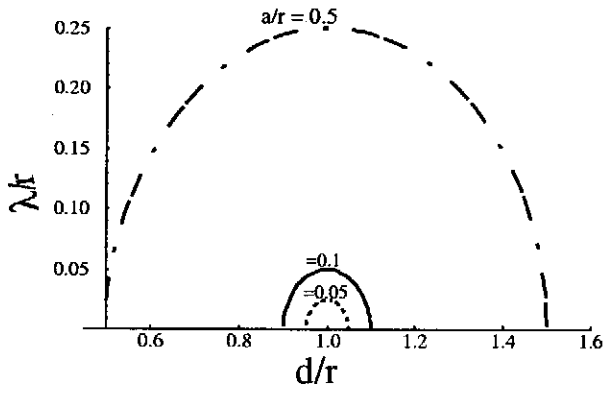

Fig. 10. Cross-field motion (λ) as a function of impact parameter (d) and relative scale of MD radius (a) and ion gyroradius (r).

O to point O''. Below we will go through the geometry to determine the distance between points O and O'' . The value "λ", the cross-field displacement, is a function of the quantities r, a and d.

To determine the exact expression of cross-field motion of the guiding center requires several figures and several geometrical calculations. Figure 9 shows Fig. 8 with the impact parameter split into two parts, "d_1", and "d_2". With a few intermediate steps it can be shown that the half chord length "l" is equal to

$$l = \left(a^2 - \left[\frac{a^2 + d^2 - r^2}{2d} \right]^2 \right)^{1/2} \tag{2}$$

From simple geometry it can be shown that:

$$\frac{\lambda}{2} = l' \left(\frac{r' - r}{r'} \right) \tag{3}$$

where l' is the half-chord length with the particle gyrocenter at point O'. The expression for l' can be given from examining Fig. 8 and using an analogous expression from Eq. 2:

$$l' = \left(a^2 - \left[\frac{a^2 + (d')^2 - (r')^2}{2(d')} \right]^2 \right)^{1/2} \tag{4}$$

where d' is the distance from O' to the center of the MD.

It can easily be shown (a number of steps are needed) that the expression for d' is:

$$d' = \left(\left[l \left(\frac{r' - r}{r} \right) \right]^2 + \left[(r^2 - l^2)^{1/2} \left(\frac{r' - r}{r} \right) + d \right]^2 \right)^{1/2} \tag{5}$$

The above four expressions give the value λ as a function of r, B_0, B_{MD}, a and d.

In Fig. 10, we illustrate the motion of the particle guiding center versus the normalized impact parameter, λ/r. λ is given for three different scale sizes of the MD: $a/r = 0.05$, 0.1 and 0.5. For all of the curves, $B_{MD}/B_0 = 0.5$. Note that the motion is finite and positive for $(1 - a/r) < d/r < (1 + a/r)$. For an impact parameter lying on the range $(-1 - a/r) < d/r < (-1 + a/r)$, the cross-field motion is in the negative direction with the same magnitudes.

Figure 11 gives the normalized cross-field motion λ/r as a function of normalized impact parameter, d/r, for various values of B_{MD}/B_0 (0.5, 0.25 and 0.1). Clearly the largest motions are associated with the case when the field magnitude change is the greatest ($B_{MD}/B_0 = 0.1$). All curves in this figure correspond to $a/r = 0.1$.

As an example of cross-field diffusion due to interactions with MDs, we use Fig. 12 (day 267, 1994), a day when there is a large number of MDs. There are approximately 10 events where $B_{MD}/B_0 < 0.2$. Thus a mean separation between MDs convected at ~ 750 km s^{-1} is $\sim 7 \times 10^6$ km. For a 1 MeV proton, $r \approx a$. It can been seen from eqs. 3 - 5 that λ_{max}, the maximum cross-field scattering distance, for a 45° pitch angle particle is one scattering (of $\lambda = a$) every 2 gyroperiod. This is an extremely rapid rate of diffusion. This, of course, is only an approximation. We have used a maxi-

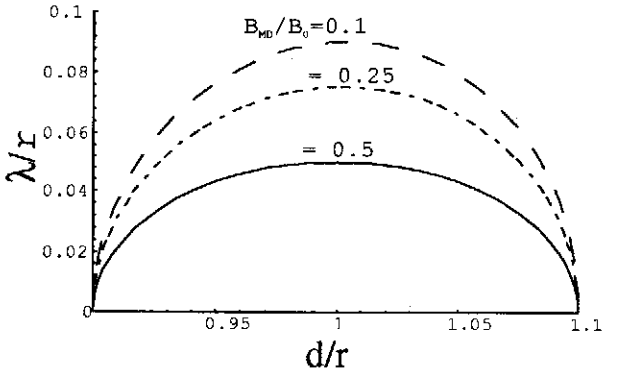

Fig. 11. Same as Fig. 10, but the various curves indicate different ratios of the magnetic field decrease (B_{MD}) to the ambient field (B_0).

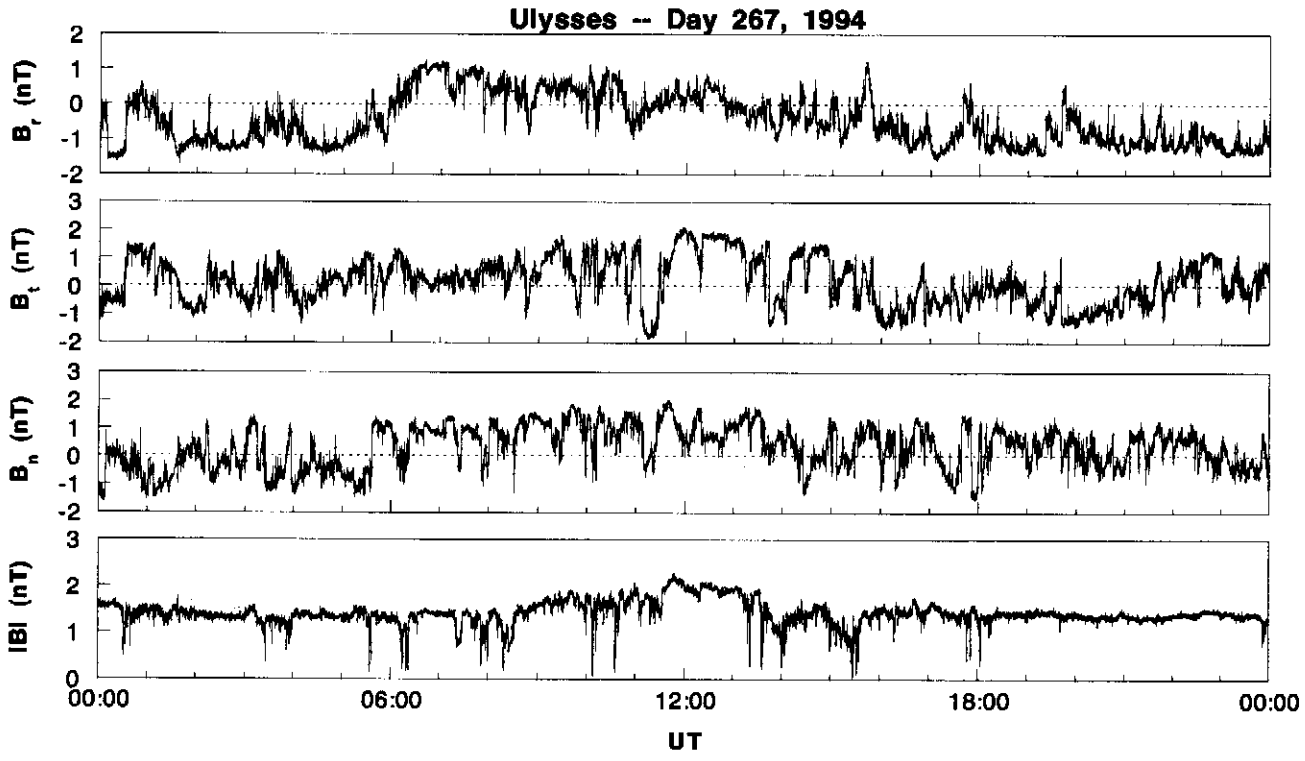

Fig. 12. The magnetic field for day 267, 1994. There are over ten events where $B_{MD}/B_0 < 0.2$.

mum rate of scattering, and the actual rate will be somewhat less. On the other hand, scattering due to interactions with MDs with larger B_{MD}/B_0 ratios was not taken into account. This will increase the cross-field diffusion rate.

3 Summary and discussion

The statistical properties of magnetic decreases at the heliospheric pole $\sim$ 2.5 AU from the sun have been presented. A generalized mathematical formulation for the amount of cross-field diffusion due to charged particle interactions with MDs has been derived. A specific example has been provided to illustrate that $\sim$ 1 MeV proton interactions with MDs can lead to very rapid cross-field diffusion.

All of the material necessary for a general cross-field diffusion model/theory are thus in place. The next steps will be to set up a Monte Carlo routine where a particle of specific energy interacts with a MD of specific size (the results of Fig. 4) with a specific (random) impact parameter and with a specific B_M value (the results of using Fig. 3) and with a measured time between interactions, Δt. The computer calculations will be repeated for particles of different energies to derive a statistical response for the interaction. This computer model is well beyond this present paper. Thus, we end our present efforts at this point.

As previously mentioned, energetic particle resonant interactions with waves lead to pitch-angle scattering, and to cross-field diffusion as a second order effect (Tsurutani and Thorne, 1982). The polar regions of the heliosphere contain nonlinear Alfvén waves, so pitch angle scattering from such interactions is expected to be intense. However, at this time we do not know what the level of cross-field diffusion will be from this process. Thus, an intercomparison of diffusion rates from the two different processes is not possible at this time. A detailed comparison will have to await further calculations on both sides.

3.1 Origin of MDs

What are the MDs and what is the mechanism for their formation? Can they be magnetic holes detected at high latitudes? Turner et al. (1977) had discovered the phenomenon of interplanetary "magnetic holes", regions of field decrease, detected in the ecliptic plane. Burlaga and Lemaire (1978) explained magnetic holes as nonpropagating, sheet-like pressure balanced equilibrium structures. The statistical properties of "linear holes", a subset of magnetic holes where the field directionality changes by less than 5° to 10°, have been discussed by Winterhalter et al. (1994, 1995). The plasmas surrounding many holes were marginally mirror-mode stable (see also Ho et al. (1995) for high latitude MDs) and the ecliptic plane holes occurred preferentially in interaction regions near the leading edges of high-speed solar wind streams. Winterhalter et al. (1995) have suggested that these linear holes may be remnants of the mirror instability.

More recently, Baumgärtel (1999) has attempted to describe magnetic holes as MHD solitary waves propagating at large normal angles to the magnetic field. He has predicted the scale size and stated that the usual soliton inverse rela-

tionship between soliton amplitude and thickness is not held, but does not specify a particular relationship.

The raw statistical results presented here (figs. 2 and 6) indicate that there is a continuum of angular changes across MDs and a continuum of normals at the MD boundaries. The continuum of normals of the discontinuities at MD boundaries argues against the idea that MDs are "dark" solitons. Also, Fig. 5 indicates that there is no relationship between the MD amplitude and width.

While previous publications (Ho et al., 1995) have suggested that some MDs may be associated with the mirror instability (linear MDs) and others with current sheets, some of us are now reassessing this point of view with the goal of searching for one mechanism which will explain all of the phenomena. The mirror mode explanation has several problems. First, it only attempts to explain part of holes/MDs. Second, the structures have very different profiles from mirror modes detected in planetary magnetosheaths (Tsurutani et al., 1982, 1993; Bavassano-Cattaneo et al., 1998), interplanetary space (Tsurutani et al., 1992) or at comets (Russell et al., 1987; Tsurutani et al., 1999). In the above mentioned regions, there are quasiperiodic oscillations in B and ρ, whereas MDs do not have such structures. Thirdly, and perhaps most importantly, high latitude MDs are bounded by discontinuities (whether or not holes detected in the ecliptic plane do or do not have such structures has not been discussed in the literature). Mirror modes detected in planetary magnetosheaths and other regions of space are not bounded by discontinuities. There is also no theoretical reason why mirror modes should be thus bounded.

Our present view is that if all MDs are due to the same generation mechanism, the correct explanation of the origin has not been offered to date. Furthermore, the relationship between high-latitude MDs and ecliptic plane magnetic holes has yet to be established. In the original work by Turner et al. (1977), magnetic hole examples did not have associated discontinuities. The further work by Winterhalter et al. (1995) did not address this important issue as well. Establishment of this important link will help unify our picture of where in the heliosphere such phenomena are occurring and will aid in our developing a picture of a generation mechanism.

Acknowledgements. Portions of this research were performed at the Jet Propulsion Laboratory, California Institute of Technology, Pasadena, under contract with the National Aeronautics and Space Administration, Washington, D.C. We wish to thank E. J. Smith for helpful scientific discussions.

References

Balogh, A., Smith, E. J., Tsurutani, B. T., Southwood, D. J., Forsyth, R. J., and Horbury, T. S., The heliospheric magnetic field over the south polar region of the sun, *Science*, *268*, 1007–1010, 1995.

Baumgärtel, K., Soliton approach to magnetic holes, to appear in *J. Geophys. Res.*, 1999.

Bavassano-Cattaneo, M. B., Basile, C., Morena, G., and Richardson, J. D., Evolution of mirror structures in the magnetosheaths of Saturn from the bow shock to the magnetopause, *J. Geophys. Res.*, *101*, 11961–, 1998.

Burlaga, L. F., and Lemaire, J. F., Interplanetary magnetic holes: Theory, *J. Geophys. Res.*, *83*, 5157–5160, 1978.

Goldstein, B. E., Neugebauer, M., and Smith, E. J., Alfvén waves, alpha particles, and pickup ions in the solar wind, *Geophys. Res. Lett.*, *22*, 3389–3392, 1995.

Ho, C. M., Tsurutani, B. T., Goldstein, B. E., Phillips, J. L., and Balogh, A., Tangential discontinuities at high heliographic latitudes ($\sim -80°$), *Geophys. Res. Lett.*, *22*, 3409–3412, 1995.

Phillips, J. L., Balogh, A., Bame, S. J., Goldstein, B. E., Gosling, J. T., Hoeksema, J. T., McComas, D. J., Neugebauer, M., Sheeley, Jr., N. R., and Wang, Y.-M., Ulysses at 50° south: Constant immersion in the high-speed solar wind, *Geophys. Res. Lett.*, *21*, 1105–1108, 1994.

Russell, C. T., Riedler, W., Schwingenschuh, K., and Yeroshenko, Y., Mirror instability in the magnetosphere of comet Halley, *Geophys. Res. Lett.*, *14*, 644–647, 1987.

Schlickeiser, R., Cosmic-ray transport and acceleration. I. Derivation of the kinetic equation and application to cosmic rays in a static cold media, *Astrophys. J.*, *336*, 243–263, 1989.

Smith, E. J., Balogh, A., Neugebauer, M., and McComas, D., Ulysses observations of Alfvén waves in the southern and northern solar hemispheres, *Geophys. Res. Lett.*, *22*, 3381–3384, 1995.

Smith, E. J. Identification of interplanetary tangential and rotational discontinuities, *J. Geophys. Res.*, *78*, 2054–2063, 1973.

Tsurutani, B. T., Smith, E. J., Anderson, R. R., Ogilvie, K. W., Scudder, J. D., Baker, D. N., and Bame, S. J., Lion roars and nonoscillatory drift mirror waves in the magnetosheath, *J. Geophys. Res.*, *87*, 6060–6072, 1982.

Tsurutani, B. T., Southwood, D. J., Smith, E. J., and Balogh, A., Nonlinear magnetosonic waves and mirror mode structures in the March 1991 Ulysses interplanetary event, *Geophys. Res. Lett.*, *19*, 1267–1270, 1992.

Tsurutani, B. T., Southwood, D. J., Smith, E. J., and Balogh, A., A survey of low frequency waves at Jupiter: The Ulysses encounter, *J. Geophys. Res.*, *98*, 21203–21216, 1993.

Tsurutani, B. T., Ho, C. M., Smith, E. J., Neugebauer, M., Goldstein, B. E., Mok, J. S., Arballo, J. K., Balogh, A., Southwood, D. J., and Feldman, W. C., The relationship between interplanetary discontinuities and Alfvén waves: Ulysses observations, *Geophys. Res. Lett.*, *21*, 2267–2270, 1994.

Tsurutani, B. T., Smith, E. J., Ho, C. M., Neugebauer, M., Goldstein, B. E., Mok, J. S., Balogh, A., Southwood, D., and Feldman, W. C., Interplanetary discontinuities and Alfvén waves, *Space Sci. Rev.*, *72*, 205–210, 1995.

Tsurutani, B. T., Lakhina, G. S., Smith, E. J., Buti, B., Moses, S. L., Coroniti, F. V., Brinca, A. L., Slavin, J. A., and Zwickl, R. D., Mirror-mode structures and ELF plasma waves in the Giacobini-Zinner magnetosheath, *Nonlinear Proc. Geophys., in press*, 1999.

Tsurutani, B. T., and Ho, C.M., A review of discontinuities and Alfvén waves in interplanetary space: Ulysses results, *Rev. Geophys.*, *37*, 517–541, 1999.

Tsurutani, B. T., and Lakhina, G. S., Some basic concepts of wave-particle interactions in collisionless plasmas, *Rev. Geophys.*, *35*, 491–502, 1997.

Tsurutani, B. T., and Thorne, R. M., Diffusion processes in the Magnetopause boundary layer, *Geophys. Res. Lett.*, *9*, 1247–1250, 1982.

Turner, J. M., Burlaga, L. F., Ness, N. F., and Lemaire, J. F., Magnetic holes in the solar wind, *J. Geophys. Res.*, *82*, 1921–1924, 1977.

Winterhalter, D., Neugebauer, M., Goldstein, B. E., Smith, E. J., Bame, S. J., and Balogh, A., Ulysses field and plasma observations of magnetic holes in the solar wind and their relation to mirror-mode structures, *J. Geophys. Res.*, *99*, 23371–23381, 1994.

Winterhalter, D., Neugebauer, M., Goldstein, B. E., et al., Magnetic holes in the solar wind and their relation to mirror-mode structures, *Space Sci. Rev.*, *72*, 201, 1995.